

# **Stress and Deformation Behaviour of Circular Tunnels situated in Rock mass**

MAJOR PROJECT II

REPORT

SUBMITTED IN PARTIAL FULFILLMENT OF THE  
REQUIREMENTS FOR THE AWARD OF THE DEGREE

OF

MASTER OF TECHNOLOGY

IN

**GEOTECHNICAL ENGINEERING**

Submitted By:

**AKASH CHANDRA MANIK**

**2k18/GTE/02**

Under the Supervision of

**Prof. AMIT KUMAR SHRIVASTAVA**



**DEPARTMENT OF CIVIL ENGINEERING**

DELHI TECHNOLOGICAL UNIVERSITY

(Formerly Delhi College of Engineering)

Bawana Road, Delhi - 110042

AUGUST, 2020

## **CANDIDATE’S DECLARATION**

I, Akash Chandra Manik, Roll No. 2K18/GTE/02, a student of M. Tech (Geotechnical Engineering), hereby declare that the report titled “Stress and Deformation behaviour of Circular Tunnels situated in Rock Mass” which is submitted by me to the Department of Civil Engineering, Delhi Technological University, Delhi, in partial fulfillment of the requirement for the award of the degree of Master of Technology, is original and not copied from any source without proper citation. This work has not previously formed the basis for the award of any Degree, Diploma, Associateship, Fellowship or another similar title of recognition.

**Place:** New Delhi

**Date:** 15<sup>th</sup> August, 2020

## **CERTIFICATE**

I hereby certify that the report titled “Stress and deformation behaviour of Circular Tunnels situated in Rock Mass” which is submitted by AKASH CHANDRA MANIK, 2K18/GTE/02, Department of Civil Engineering, Delhi Technological University, Delhi in partial fulfillment of the requirement for the award of the degree of Master of Technology, is a record of the project work carried out by the student under my supervision. To the best of my knowledge this work has not been submitted in part or full for any Degree or Diploma to this University or elsewhere.

**Place:** New Delhi

**Prof. AMIT KUMAR SHRIVASTAVA**

**Date:** 15<sup>th</sup> August, 2020

**SUPERVISOR**

## **ACKNOWLEDGMENT**

I wish to express my profound gratitude and indebtedness to **Prof. AMIT KUMAR SHRIVASTAVA**, Professor, Department of Civil Engineering, Delhi Technological University, New Delhi, for introducing the present topic and for his inspiring guidance, constructive criticism and valuable suggestions throughout this project work.

I would also express my gratitude to all the professors of the Department of Civil Engineering, Delhi Technological University, New Delhi, for their guidance and the support they have provided me.

Lastly, my sincere thanks to all of my friends, Mr. Parvesh Kaushal (PhD scholar) and lastly, parents who have patiently extended all sorts of help for accomplishing this undertaking.

AKASH CHANDRA MANIK

2k18 / GTE / 02

Department of Civil Engineering

Delhi Technological University, New Delhi

## **ABSTRACT**

Increasing use of Tunnels for underground roadways, metro rail or railways makes it an important area for study. Construction of tunnels through the rock or soil mass would require the determination of induced stresses and deformation resulting from in situ stress conditions. This thesis involves study of the theoretical solutions provided by various researchers related to stress and deformation around a circular tunnel and a comparison among them simultaneously for stresses and strains keeping certain parameters constant around the tunnel. This has been carried out in two steps. First step involves casting and model testing in the laboratory to evaluate stress and strain induced in the model under uniaxial loading. This has already been carried out by Kumar, P. and the final readings of that model test have been adopted directly for further analysis. The salient features of this experiment are, experimental model of circular tunnel casted using Perspex box specially designed to act as a mould. Plaster of Paris was used as the casting material to simulate weathered rock mass. Strain gauges were attached at the tunnel periphery at specific intervals. Second step involves comparing the various solutions given by researchers using ultimate load as the input from the model testing and computing stresses and corresponding strain values analytically considering the plane stress and plane strain condition for stresses and strains respectively. Deformation profiles, stress vs strain curves for different solutions were obtained for further study and conclusions were drawn.

# TABLE OF CONTENTS

Candidate's Declaration	i
Certificate	ii
Acknowledgement	iii
Abstract	iv
List of Figures	
List of Tables	
<b>CHAPTER 1</b>	
1.1 Introduction	1
1.2 Objectives of research	2
1.3 Methodology adopted	2
<b>CHAPTER 2</b>	
2.1 Literature Review	4
<b>CHAPTER 3</b>	
3.1 Various analytical solutions	8
3.1.1 Kirsch (1898) Solutions	9
3.1.2 Bray (1967) Solutions	11
3.1.3 Pender (1980) solutions	13
3.2 Trial curves	14
3.2.1 Kirsch (1898) Solutions	14
3.2.2 Bray (1967) Solutions	16
3.2.3 Pender (1898) Solutions	16
<b>CHAPTER 4</b>	
4.1 Experimental Setup	20
4.1.1 Perspex Box design	21
<b>CHAPTER 5</b>	
5.1 Conduction of experiment	23

5.2 Analytical Results	23
5.2.1 Kirsch (1898) Solutions	23
5.2.2 Bray (1967) Solutions	25
5.2.3 Pender (1898) Solutions	26
5.3 Graphical comparison of analytical results	27
5.3.1 Stress comparison	28
5.3.2 Deformation comparison	29

## **CHAPTER 6**

6.1 Analytical result curves	30
6.2 Stress v/s Strain	32
6.3 Deformation Profile	34

## **CHAPTER 7**

7.1 Conclusion	35
----------------	----

## **REFERENCES**

## LIST OF TABLES

---

<b>Table 5.1</b> Maximum induced stress values	23
<b>Table 5.2</b> Nomenclature	24
<b>Table 5.3</b> Stress values for 3cm model	24
<b>Table 5.4</b> Stress values for 5cm model	25
<b>Table 5.5</b> Displacement Values	18
<b>Table 5.6</b> Stress values for 3cm model	26
<b>Table 5.7</b> Stress values for 5cm model	26
<b>Table 5.8</b> Displacement Values	27



## LIST OF FIGURES

---

<b>Fig. 3.1</b>	– Stress coordinates in a circular plate located at infinite depth	8
<b>Fig. 3.2</b>	– Co-ordinate system for stresses and deformation in circular hole	9
<b>Fig. 3.3</b>	– Variation of Radial and circumferential stress along x and y direction	15
<b>Fig. 3.4</b>	– $\frac{Eu(a)}{\sigma_{va}}$ v/s $\theta$ & $\frac{Ev(a)}{\sigma_{va}}$ v/s $\theta$	16
<b>Fig. 3.5</b>	Variation of Radial and circumferential stress along x and y direction	17
<b>Fig. 3.6</b>	$\frac{Eu(a)}{\sigma_{va}}$ v/s $\theta$ & $\frac{Ev(a)}{\sigma_{va}}$ v/s $\theta$	18
<b>Fig. 4.1</b>	Schematic diagram of Perspex box	21
<b>Fig. 4.2</b>	Front view and cross section @ X-X	22
<b>Fig. 4.3</b>	Load setup of a circular tunnel model	22
<b>Fig. 5.1</b>	(a) 5cm Tunnel (Table 5.4)	28
	(b) 5cm Tunnel (Table 5.7)	28
<b>Fig. 5.2</b>	(a) 3cm Tunnel (Table 5.3)	28
	(b) 3cm Tunnel (Table 5.6)	28
<b>Fig. 5.3</b>	(a) 5cm Tunnel (Table 5.5)	29
	(b) 5cm Tunnel (Table 5.8)	29
<b>Fig. 5.3</b>	(a) 3cm Tunnel (Table 5.5)	29
	(b) 3cm Tunnel (Table 5.8)	29

<b>Fig. 6.1</b>	(a) $\sigma_r$ v/s time	30
	(b) $\sigma_\theta$ v/s time	30
	(c) $\tau_{r\theta}$ v/s time	30
<b>Fig. 6.2</b>	(a) $\sigma_r$ v/s time	30
	(b) $\sigma_\theta$ v/s time	30
	(c) $\tau_{r\theta}$ v/s time	30
<b>Fig. 6.3</b>	(a) $\sigma_r$ v/s time	31
	(b) $\sigma_\theta$ v/s time	31
	(c) $\tau_{r\theta}$ v/s time	31
<b>Fig. 6.4</b>	(a) $\sigma_r$ v/s time	31
	(b) $\sigma_\theta$ v/s time	31
	(c) $\tau_{r\theta}$ v/s time	31
<b>Fig.6.5</b>	(a) Stress v/s strain trend (3cm tunnel)	32
	(b) Stress v/s strain trend (5cm tunnel)	32
<b>Fig. 6.6</b>	Percentage variation in strain with experimental readings	32
<b>Fig. 6.7</b>	(a) $E_u$ v/s $\theta$	34
	(b) $E_v$ v/s $\theta$	34

# CHAPTER 1

---

## 1.1 Introduction

The use of tunnels for various commute and other purposes like Railways, Metro rails and sewage transport is surmounting exponentially as the surface land is nearing its saturation limit. Construction of massive concrete structures will soon cover the land to its maximum capacity. Due to this growing concern for the near future, tunnels are of importance. To facilitate the construction of tunnels, one must possess a fair idea about the causes of stress generation, mode of transmission, soil-structure interaction i.e. Soil/Rock and tunnel lining interaction, the deformations due to the loads at various locations, the modes of failure and many other important aspects. The primary source of stresses exerted at the tunnel periphery is due to the vertical overburden pressure and lateral pressure is exerted due to the at rest condition of the adjoining rock mass. It can be stated that the vertical overburden pressure may be due to the soil existing over the underground space and the surcharge applied at the ground level in the vicinity of the tunnel periphery within the influence zone.

Tunnels are predominantly subjected to 3 types of loads which needs to be taken into account while designing the lining material and while accounting for permissible settlement as per guidelines. Loads acting are mainly classified into:

- Static Load resulting due to overburden mass of soil / rock
- Dynamic load generated due to movement of metro rail or heavy machinery
- Impact loads due to earthquakes and blasting

These loads tend to induce Bending moment, Shear force and Normal forces in the tunnel lining material which may be tensile or compressive in nature. The nature of these induced forces depends purely on the geometry and stresses acting at the tunnel periphery. Another important aspect for tunnel designers is deformation. Deformation may be radial or circumferential in nature. It must be kept in mind that the net deformation of the tunnel periphery must be within the permissible limits of ground movement. Excess deformations may lead to accidents and even settlements of super structure in some cases and ultimately collapse of structures. Hence, the estimation of stresses and deformations plays an important role in understanding the behavior of these induced forces. These induced stresses can be used further for plotting the stress paths which would indicate the state of rock / soil mass

with respect to the Mohr's failure envelope. This would aid in locating critical stress points along the periphery of the tunnel which needs special attention.

Another aspect is to assess the stability of tunnels. Stability of tunnels mainly depends upon the relative position of tunnel and construction procedure adopted. For determination of stresses, various theoretical formulations have been proposed over the past years to determine the stresses and deformation in a tunnel. It is to be noted that within the scope of this study, the adjoining mass around the tunnel periphery is assumed to be weathered rock mass and the term 'soil' is used interchangeably with rock mass unless specifically mentioned otherwise. Though the extensive use of analytical solutions is no longer a usual preference due to the emergence of computers and numerical codes which are faster, more efficient and accurate. Still analytical solutions have their relevance as they serve as a reference benchmark for the results of numerical analysis. Moreover, they are useful in identifying problem variables and can provide some simple results which can be applied effortlessly.

## **1.2 Objectives of Thesis**

1. To understand the stress pattern around the tunnel periphery caused due to the overhead loading using analytical approach.
2. To understand the deformation pattern around the tunnel periphery due to overhead loading using analytical approach.
3. Comparative study among the different solutions for both stresses and deformations in case of circular tunnel to observe the similarities and differences.
4. Graphical representation of the stresses and strains and analysis of graphs.

## **1.3 Methodology adopted**

Tunneling is inherently a 3-D problem and hence, must be ideally modeled as such. However, the approach of plane strain wherein, the a 3D problem is conveniently reduced to a 2D problem by assuming  $\epsilon_3 = 0$  *i.e.* strain along z axis (longitudinal) is neglected, is assumed for this study as it reduces a complex 3D problem to a set of simple equation, which are easier to handle. The thesis is completed in the following steps:

- 1) Review of existing theories for the analysis of tunnels in order to choose the most appropriate solution within the scope of this study.
- 2) Obtaining the stress and displacement magnitudes along with their nature using various analytical solutions.
- 3) Study the results from Step 2 and understand the differences and their causes.

## CHAPTER 2

---

### 2.1 Literature Review

The analysis over tunnels can be broadly classified into physical or experimental, numerical and analytical. Construction of a tunnel primarily involves choosing a suitable method for each individual project as every project is unique. The choice of this method depends on the traits of the project. It should also cater to the purpose for which the tunnel is being made efficiently and should make use of the useful space above and under the ground while minimizing the negative effects due to its construction such as excessive settlements or ground movement. Depending on whether it is a metro or a highway, various construction techniques are used.

In case of metro construction, the main construction methods are Cut and Cover method, New Austrian Tunnelling Method, Shield Method. Various new innovative methods are being introduced which are combination of the methods mentioned above. In Cut and Cover method, the excavation takes place from up-to-down starting from basement of the tunnel to the desired elevation. Afterwards, backfilling of foundation pit to restore the ground is carried out. They are further classified into unsupported slope excavation and supported foundation pit excavation based on whether the side wall reinforcement is provided or not. This method of construction leads to economical design and delivers a well stressed main body of the tunnel. It is primarily chosen when there is no restriction on ground traffic movement and environment as the construction can be achieved as and when needed. It is to be avoided when there is a primary traffic route as it will block the same for a long time. Also, this choice of method is not appropriate when construction is to take place in the vicinity of a residential zone as it produces great noise and vibrations. Many scientific developments have been made in cut and cover method of tunnel construction (Guo (2019)). New Austrian Tunnelling method (NATM) (Xiao et al. (2009)) is principally the application of rock mechanics theory based on maintaining and utilizing the self-supporting capacity of the surrounding rock. The surrounding rock acts as the primary support system. The construction process involves in six steps *i.e.* line positioning ; drilling, loading and blasting; dust removal by ventilation; anchor and steel arch support followed by bar mat reinforcement; shotcreting to form the preliminary bracing; building the concrete as the secondary lining. The main advantage of NATM is the elimination of supporting material as

it makes use of the surrounding structure extensively. Another important trait of this method is its low cost. NATM can be preferred for tunnel construction in weak surrounding rock, poor geology conditions and shallow tunnels. Scientific development in the field of NATM are quite a few (Guo (2019)). Construction of tunnels using NATM and by TBM have been discussed in detail (Phadke et al. (2017)). Shield method is the most widely used method in subway construction around the world. Tunnel Boring Machine (TBM) is used in this technique. A TBM consists of a shield and trailing support mechanism. Excavation of soil at the front face of the tunnel is done using shield and excavated waste is removed through machinery as either slurry or left as it is depending on the type of TBM. Hydraulic Jacks are used to push the TBM forward. An erector is used to pick-up precast concrete segments and place in the designated location to form the tunnel lining. The shield method is executed in five steps which are as follows: excavating foundation pit or constructing vertical shaft at both starting and end of the tunnel; soil excavation; TBM advancement and correction to deviation; assembling the lining material; pressing the lining material. Various developments in shield method are well presented (Guo (2019)). If the tunnel is constructed is to be carried out for a highway, various methods adopted around the world are Mining method, Shield method, Immersed tube method (He, Wang (2013)). The mining method is based on drilling and blasting excavation method. Various excavation methods available are full face excavation method, bench cut methods. These methods improved the stability of the surrounding rock mass. Another development in tunnel construction technology is the Norway tunnel Method (NTM) (Barton et al. (1974); Barton et al. (1992)) which is complementary to the NATM. The basic difference between NTM and NATM is the rock classification system adopted. NTM uses Q-system of classification of rock. High performance materials are applied as a permanent support, with secondary lining only if required in conditions such as leakage, frost and other hazardous conditions. Another advancement in tunneling technology appeared in the year 2000, the New Italian Tunnelling method (NITM) (Lunardi (2000)) which is an enhancement in the traditional NATM with addition of pressure arch theory. NITM is widely used in highway and railway tunnel designing. The Immersed tube tunnel is a commuting carrier tunnel which excavates a groove under the water of the sea, river or channel where the tunnel is to be constructed. Sections are floated to the site followed by related construction required to combine the individual segments into a whole and finally build road for traffic (Wang (1997)).

Over the past few decades, the advancement in computational power has led to development of multiple computer codes which can be implemented in studying the behavior

of structures, their response to different loading and many more. Moreover, numerical analysis is fast and accurate to some degree. The most important use of numerical analysis has been observed in the field of 3-dimensional analysis. Various numerical simulations are present comprising of various types of analysis and various constitutive models. One can choose among these options to suit the needs of the project. A comparative comprehensive study had been performed which consists of more than 60 case histories published over the last two decades which compares the numerical results with field measurements and also, shows the performance of numerical modelling in tunneling in terms of ground displacement and lining loads (Negro et al. (2000)). The research evaluates the various case studies in the lines of physical as well as numerical aspects. Physical aspect involves classifying the case studies based on the construction method adopted for each case i.e. Side drift, shield, NATM, Mined, Open shield, Slurry shield etc. Numerical aspects were also considered for each case and all the cases are classified into type of analysis i.e. 2-D or 3-D, numerical simulation used, such as Stress reduction, imposed convergence, Core removal etc. , choice of constitutive model chosen i.e. Elastic, Non- Linear elastic, Elastoplastic in which yield and failure surface were coinciding or distinct yield and failure surface. The research also classified the computed code on the basis of method of analysis used i.e. Finite element analysis and Finite difference method.

Analytical approach is adopted initially before deciding the appropriate method of construction of tunnel or method of numerical analysis to be adopted. This serves as the guideline to check for results with physical and numerical modelling. The only drawback of this approach is that it is time consuming and involves complex solutions which can be analytically challenging to solve. In the theory of plane elasticity which assumes the material to be isotropic and homogeneous, when the variation of body forces is ignored , the same stress distribution is obtained for both plane stress and plane strain by the solution of boundary value problems in which, only the surface tractions are specified (Malvern 1969). Therefore, elastic stress distribution around a deep tunnel can be approximated by that of a hole having the same shape as the tunnel and situated in an infinitely large and elastic plate subjected to end loads. The classical solutions for stresses around a hole in an infinite plate were applied extensively to the early studies on the stresses around underground openings (Terzaghi et al. (1952); Obert et al. (1960)). Stress distribution around a circular hole in a uniaxially loaded plate has been considered perhaps the single most important problem in the field of rock mechanics (Jaeger et al. (1976)). The solution to this problem is known as Kirsch Solution (Kirsch (1898)), which is widely applied for the design of circular tunnels



and shafts. Similarly, Inglis's Solution for the ellipse (Inglis (1913)) had multiple applications which further lead to emergence and development of fracture mechanics. Greenspan's solution for the ovaloid (Greenspan (1944)) is another example of classical "hole in plate" solutions. Closed form solution for determination of stresses in conventionally used tunnel shapes having arched roof and a vertical symmetry axis have been presented (Gercek (1997)). Analytical solutions have also been presented for stresses and displacements in a semi-infinite elastic ground subjected to surcharge loading for twin tunnels (H.N Wang et al (2017)). The simplicity of the elastic solution for the stresses and displacements around a deep circular opening provides great preliminary insight into the significance of various parameters (Muir et al. (1975); Curtis (1976)).

Even though it is known that the actual deformation behavior of the soil during tunneling operation is not plain, the assumption of plain strain is made for the sake of simplicity. A tunnel is regarded as 'deep' if the free surface does not significantly affect the stresses and displacement around the opening. This is a reasonable approximation for the depth greater than several tunnel diameters. For the scope of this research, only deep circular tunnel is considered for study.

## CHAPTER 3

### 3.1 Various Analytical solutions for Circular Tunnel

Over the decades, various theories have been presented by researchers across the world for the case of circular hole situated in a plate of infinite extent. It is assumed that the stresses applied act at the distant boundary as shown in the Fig. 3.1

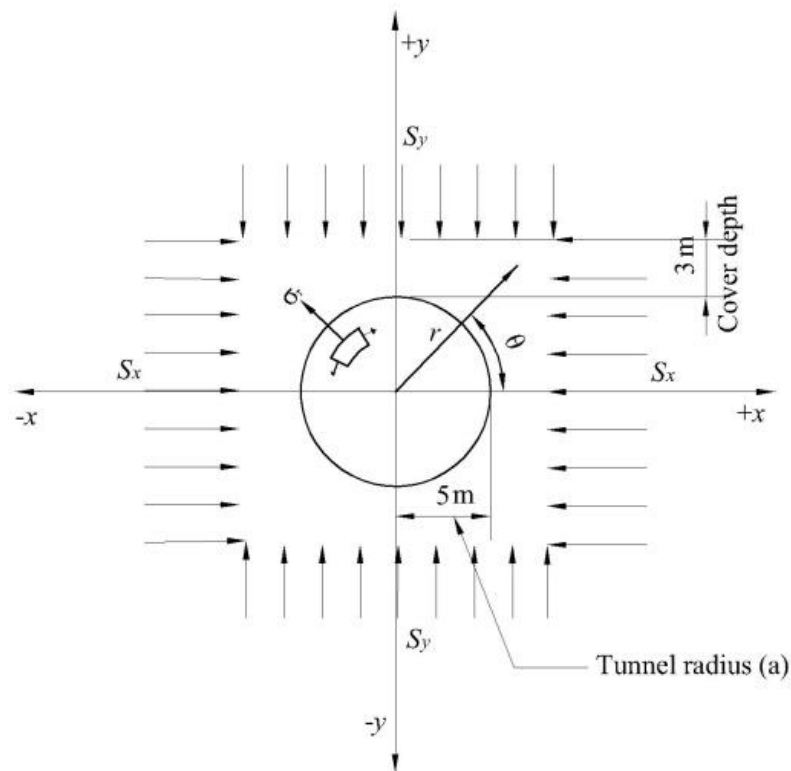


**Fig. 3.1** Coordinate System adopted for Circular hole situated in an infinite plate

The following nomenclature has been used:

Circular hole radius =  $a$

Applied Stress along  $x$ -direction =  $S_x$

Applied Stress along  $y$ -direction =  $S_y$

Radial distance =  $r$  (from the center of the circle)

Angle subtended by the radial axis from  $+x$  axis =  $\theta$  (anticlockwise sense)

Radial stress =  $\sigma_r$

Tangential stress =  $\sigma_\theta$

Shear stress =  $\tau_{r\theta}$

The equations for obtaining stresses are given as follows:

$$\sigma_r = \frac{1}{2} \left\{ (S_x + S_y) \left[ 1 - \frac{a^2}{r^2} \right] + (S_x - S_y) \left[ 1 + \frac{3a^4}{r^4} - \frac{4a^2}{r^2} \right] \cdot \cos(2\theta) \right\} \quad (3.1)$$

$$\sigma_\theta = \frac{1}{2} \left\{ (S_x + S_y) \left[ 1 + \frac{a^2}{r^2} \right] - (S_x - S_y) \left[ 1 + \frac{3a^4}{r^4} \right] \cdot \cos(2\theta) \right\} \quad (3.2)$$

$$\tau_{r\theta} = -\frac{1}{2} (S_x - S_y) \left[ 1 - \frac{3a^4}{r^4} + \frac{2a^2}{r^2} \right] \cdot \sin(2\theta) \quad (3.3)$$

### 3.1.1 Kirsch (1898) Solutions

Kirsch (1898) derived the solution for stress distribution around a circular hole. The original theory assumed a circular borehole situated in a very large plate subjected to remotely uniform tensile stresses. The same solutions can be adopted for circular tunnels situated in rock mass with little manipulations for uniaxial stress state. Assumptions are as follows:

1. The circular hole is situated in a plate which extends infinitely (very large).
2. Plane strain condition exists. (to reduce the complexity from 3D to 2D plane)
3. The rock material surrounding the tunnel is continuous, homogeneous, isotropic and linearly elastic i.e. rock material is stressed within the elastic range.

Considering an Uniaxial stress analysis, Let  $S_x = 0$  but  $S_y \neq 0$ , which reduces the current problem to plane stress problem. The above equations (3.1), (3.2) and (3.3) transforms into:

$$\sigma_r = \frac{1}{2} \cdot S_y \cdot \left\{ \left[ 1 - \frac{a^2}{r^2} \right] - \left[ 1 + \frac{3a^4}{r^4} - \frac{4a^2}{r^2} \right] \cdot \cos(2\theta) \right\} \quad (3.4)$$

$$\sigma_\theta = \frac{1}{2} \cdot S_y \cdot \left\{ \left[ 1 + \frac{a^2}{r^2} \right] + \left[ 1 + \frac{3a^4}{r^4} \right] \cdot \cos(2\theta) \right\} \quad (3.5)$$

$$\tau_{r\theta} = \frac{1}{2} \cdot S_y \cdot \left[ 1 - \frac{3a^4}{r^4} + \frac{2a^2}{r^2} \right] \cdot \sin(2\theta) \quad (3.6)$$

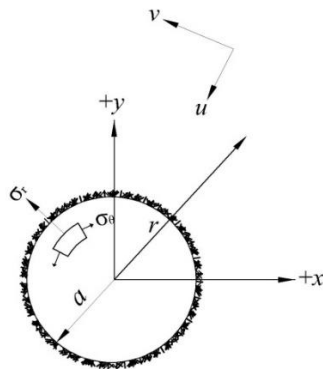


**Fig. 3.2** Coordinate System for stresses and deformation in a circular hole

The solutions given by Kirsch (1898) can be expressed as in Eqs. {(3.4),(3.5),(3.6)} . Some of the important observations derived from Eqs. {(3.4), (3.5), (3.6)} are as follows:

- The Maximum Tangential stress is 3 times the applied stress and occurs at the boundary on the x axis, *i.e.* at  $\theta = 0$  or  $\pi$
- When the angle of inclination  $\theta = \frac{3\pi}{2}$  or  $\frac{\pi}{2}$ , the tangential stress at the boundary of the opening is equal to the applied stress but is of opposite sign.

The stress displacement relation for plain stresses may be then defined as:

$$\epsilon_r = \frac{\partial u}{\partial r} = \frac{1}{E} (\sigma_r - \nu \cdot \sigma_\theta) \quad (3.7)$$

$$\epsilon_\theta = \frac{u}{r} + \frac{1}{r} \frac{\partial v}{\partial \theta} = \frac{1}{E} (\sigma_\theta - \nu \cdot \sigma_r) \quad (3.8)$$

$$\gamma_{r\theta} = \frac{1}{r} \frac{\partial u}{\partial \theta} + \frac{\partial v}{\partial r} - \frac{v}{r} = \frac{2(1+\nu)}{E} \tau_{r\theta} \quad (3.9)$$

Similarly, the displacement equations for plain strain case can be written as:

$$Eu = \frac{1}{2} S_y [1 - \nu^2] \left\{ \left[ r + \frac{a^2}{r} \right] - \left[ r - \frac{a^4}{r^3} + \frac{4a^2}{r} \right] \cdot \cos(2\theta) - \nu[1 + \nu] \cdot \frac{1}{2} S_y \cdot \left\{ \left[ r - \frac{a^2}{r} \right] + \left[ r - \frac{a^4}{r^3} \right] \cdot \cos(2\theta) \right\} \right\} \quad (3.10)$$

$$Ev = \frac{1}{2} S_y \cdot \left\{ [1 - \nu^2] \left[ r + \frac{2a^2}{r} + \frac{a^4}{r^3} \right] + \nu[1 + \nu] \left[ r - \frac{2a^2}{r} + \frac{a^4}{r^3} \right] \right\} \sin(2\theta) \quad (3.11)$$

In Eqs. {(3.10),(3.11)},  $u$  is the displacement coordinate in radial direction and  $v$  is the displacement coordinate in tangential direction respectively and both  $u$  and  $v$  are defined as the function of  $\theta$ ,  $\frac{a}{r}$  so it changes with angle  $\theta$  and the radial distance from the tunnel center.

It can be stated from Equations (3.10) & (3.11) that the radial displacement is maximum at

$$\theta = \frac{3\pi}{2} \text{ or } \frac{\pi}{2} .$$

If we substitute  $r = a$  in Eqs. {(3.10), (3.11)} *i.e.* which is at the tunnel periphery, we obtain:

$$Eu = [1 - \nu^2] \cdot a \cdot [S_y - 2 \cdot S_y \cdot \cos(2\theta)] \quad (3.12)$$

$$Ev = 2 \cdot [1 - \nu^2] \cdot a \cdot [S_y \cdot \sin(2\theta)] \quad (3.13)$$

The limitations to Kirsch (1898) solutions are as follows:

1. The assumption that plate extends infinitely is unrealistic as in practicality, the rock mass extends to a finite depth.
2. The assumption of plain strain condition even though reduces the 3-dimensional problem to a 2-dimensional one, is not accurate as in practicality, a tunnel situated in rock mass is a 3D problem.
3. Corrections or remarks to the results obtained by plain strain condition for 3D has not been provided or 3D has not been taken into account.
4. The assumption of rock mass being continuous, homogenous is not correct as rocks are accompanied by fissures and joints. Hence, are discontinuous structures with a little continuity in case of intact rock mass.
5. The assumption that rock mass is isotropic and linearly elastic does not stand true as rock mass is anisotropic in nature and does not follow linear elasticity.

### 3.1.2 Bray (1967) Solutions

This model was proposed by Bray (1967). It states that when the tunnel is situated in weak rock, the stress developed exceeds the yield strength and hence formation of both elastic and plastic zone occurs around the tunnel periphery. The plastic zone is also known as *yield zone*. If  $r_o$  is the radius of the tunnel and  $r_p$  is the radius of the plastic zone.

Assumptions made are as follows:

1. The rock has been assumed as weak.
2. The stress around the tunnel periphery exceeds the yield strength of the rock mass.
3. Formation of yield zone takes place.
4. The rock mass is assumed to possess homogeneity, isotropic and continuous.
5. Tangential stress is negligible and hence ignored.
6. The stresses are independent of the orientation from abscissa and radial distance and depend only on the inherent property of the rock mass.

Nomenclature used is as follows:

$\phi$  = angle of internal friction

c = cohesion

$P_o$  = In situ stress considered

Stress equations are given as:

$$\sigma_r = m_3.r.(m_1 - m_2) \quad (3.14)$$

$$\sigma_\theta = m_4.r.(m_1 - m_2) \quad (3.15)$$

Where symbols have usual meaning. Parameters  $m_1$  ,  $m_2$  ,  $m_3$  and  $m_4$  are defined as:

$$m_1 = \frac{2 \cdot \sin \phi}{1 - \sin \phi} \quad (3.16)$$

$$m_2 = c \cdot \cot \phi \quad (3.17)$$

$$m_3 = \frac{m_2}{r_0 \cdot m_1} \quad (3.18)$$

$$m_4 = m_3 \left[ \frac{1 - \sin \phi}{1 + \sin \phi} \right] \quad (3.19)$$

Also, the plastic zone radius  $r_p$  is defined by the equation:

$$r_p = a \cdot \left\{ [P_0 + c \cdot \cot \phi] \left[ \frac{1 - \sin \phi}{c \cdot \cot \phi} \right] \left[ \frac{1 - \sin \phi}{2 \cdot \sin \phi} \right] \right\} \quad (3.20)$$

Limitations to Bray (1967) solutions:

1. The rock has been assumed as weak and hence this solution is not applicable for rocks with considerable strength.
2. Yield zone formation is predetermined whereas in practicality, yielding does not necessarily take place.
3. The assumption of rock mass being continuous, homogenous is not correct as rocks are accompanied by fissures and joints. Hence, are discontinuous structures with a little continuity in case of intact rock mass.
4. The assumption that rock mass is isotropic and linearly elastic does not stand true as rock mass is anisotropic in nature and does not follow linear elasticity.
5. It has been assumed that the stresses are independent of orientation from abscissa and radial distance from center of the tunnel. It means stress magnitude is same throughout the periphery and doesn't change in magnitude which is not true.
6. It has been assumed that stresses depend only on properties of the surrounding rock mass. But in practicality, the in-situ overlaying rock weight, surcharge due to imposed loads needs to be taken into account. Even the lateral pressure exerting due to the rock mass is to be considered.

### 3.1.3 Pender (1980) Solution

Pender (1980) derived the solutions for circular hole situated in a prestressed medium where the displacements are significant at the tunnel cross section and fades out with distance from the tunnel periphery. It is also assumed that the incremental stress changes are the major causes for the displacements. The assumptions made are as follows:

1. The tunnel is excavated in a prestressed medium.
2. The displacements are maximum at the tunnel cross-section and keeps decreasing as the radial distance increases beyond the tunnel periphery.
3. Induced incremental stresses act the distant boundary of an infinite plate.
4. Incremental stress induced at boundary are the only cause of deformation.

The solutions provided are for estimation of change in stress due to increase in surface load magnitude (provided plain strain condition is satisfied) are as follows:

$$\Delta\sigma_r = -\frac{1}{2} S_y \cdot \left\{ \left[ \frac{a^2}{r^2} \right] - \left[ \frac{3a^4}{r^4} - \frac{4a^2}{r^2} \right] \right\} \cos(2\theta) \quad (3.21)$$

$$\Delta\sigma_\theta = \frac{1}{2} S_y \cdot \left\{ \left[ \frac{a^2}{r^2} \right] + \left[ \frac{3a^4}{r^4} \right] \cos(2\theta) \right\} \quad (3.22)$$

$$\Delta\tau_{r\theta} = -\frac{1}{2} S_y \cdot \left[ \frac{3a^4}{r^4} - \frac{2a^2}{r^2} \right] \sin(2\theta) \quad (3.23)$$

The Displacement caused at the tunnel periphery due to the stresses acting can be given by assuming identical assumptions as in {Kirsch (1898)} *i.e.* Only Uniaxial stresses exist and lateral stresses are ignored in the analysis:

$$Eu = \frac{(1+\nu)}{2} \cdot a \cdot S_y \cdot [1 - [3 - 4\nu] \cdot \cos 2\theta] \quad (3.24)$$

$$E\nu = \frac{(1+\nu)}{2} \cdot [3 - 4\nu] a \cdot S_y \cdot \sin(2\theta) \quad (3.25)$$

Limitation to Pender (1980) solutions:

1. The tunnel is situated in a prestressed medium. This assumption leads to deformation solutions which account only for the incremental stress. In practicality, incremental stress along with in-situ overburden cause stresses around the tunnel periphery. Hence, in-situ stresses are to be considered for more accuracy.
2. The incremental loading is assumed to act at a distant boundary which is an ideal situation and leads to far-field stresses. In practicality, the rock mass is finite in depth.

3. Lateral pressure and overburden are not considered for deriving the solution.

### 3.2 Trial Curves

Trial curves depict the variation of stress distribution around the circular tunnel. The variation is further compared with each other. The main reason for consideration of these curves is the assumption of lateral stresses. For the comparison of analytical results, lateral pressure is assumed to be non-existent due to the uniaxial assumption. These curves have been obtained by adopting sample values to the Eqs. by Kirsch (1898) and Pender (1980).

#### 3.2.1 Kirsch (1898) Solutions

Solutions provided by Kirsch were divided into 2 cases. Case I deals with trial curves depicting stress function and Case II deals with trial curves depicting displacement function in terms of  $Eu$  and  $Ev$ .

**Case I:** Stress functions using Eqs. {(3.4), (3.5), (3.6)} are discussed in this case. Trial curves are obtained for:

- 1)  $\frac{\sigma_{\theta}}{S_y} \text{ v/s } \frac{r}{a}$
- 2)  $\frac{\sigma_r}{S_y} \text{ v/s } \frac{r}{a}$

Varying  $r/a$  values have been assumed from 1 to 5 (note that the magnitude and influence of stress becomes irrelevant beyond  $r/a = 4$  *i.e.* when radial distance becomes 4 times the tunnel radius (Obert, Duvall (1967))). Hence, stresses beyond it can be ignored without compromising the accuracy of the curves. But for the smoothness and continuity of the curve, values till  $r/a = 5$  are considered as a part of extrapolation. The Tunnel radius ( $a$ ) is assumed to be 5m. The cover depth was assumed as 3m.

$S_x = 0 \text{ kN/m}^2$  *i.e.* Horizontal applied stress is assumed to be negligible, so the case is representing a Uniaxial case where the only pressure acting is the vertical stress due to overburden and surcharge and the confining pressure due to lateral earth is neglected. By adopting the already mentioned assumption, the complex problem at hand reduces to a much simple problem which is easier to handle. Equations {(3.4), (3.5) & (3.6)} are used to calculate the stress component corresponding to different  $r/a$  values and different  $\theta$  values.

$\theta$  has been varied from  $0^0$  to  $90^0$  as the tunnel under analysis is a circular tunnel and



there lies a symmetry among the 4 quadrants each having a varying  $\theta$  value from  $0^\circ - 90^\circ$ ,  $90^\circ - 180^\circ$ ,  $180^\circ - 270^\circ$ ,  $270^\circ - 360^\circ$ . Hence, only 1<sup>st</sup> Quadrant is considered for this purpose.

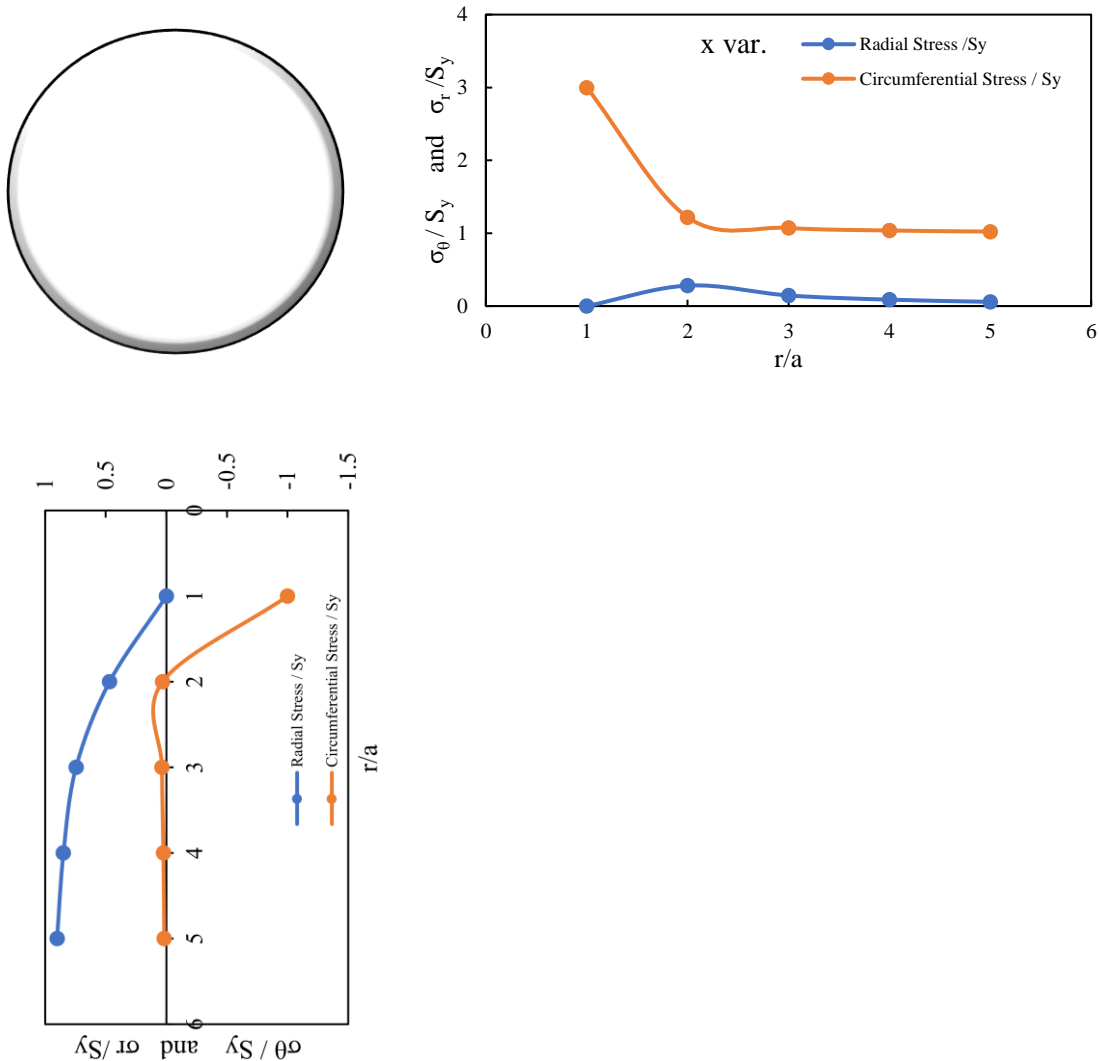


**Fig. 3.3** Variation of Radial and Circumferential Stresses along x and y direction

**Case II** Displacement functions using Eqs. {(3.12), (3.13)} are discussed in this case. Curves are obtained for:

1.  $Eu(a) / \sigma_v(a)$  v/s  $\theta$
2.  $Ev(a) / \sigma_v(a)$  v/s  $\theta$

Assumptions made in the calculation for  $u$  and  $v$  (displacement component in  $x$  and  $y$  direction) using equations (3.12) and (3.13) are;

Poisson's ratio  $\nu = 0.2$

Vertical stress  $S_y = 20 \text{ kN/m}^2$ ;

Horizontal Stress  $S_x = 10 \text{ kN/m}^2$

And radius of the tunnel ( $a$ ) = 5 m & all the displacements are calculated at the boundary interface of the tunnel *i.e.* at  $r = a$ . Sign convention is taken as follows:

- Radial displacement  $u$  is positive when it is directed towards the tunnel (●)
- Circumferential displacement  $v$  is positive in the anticlockwise direction (●)

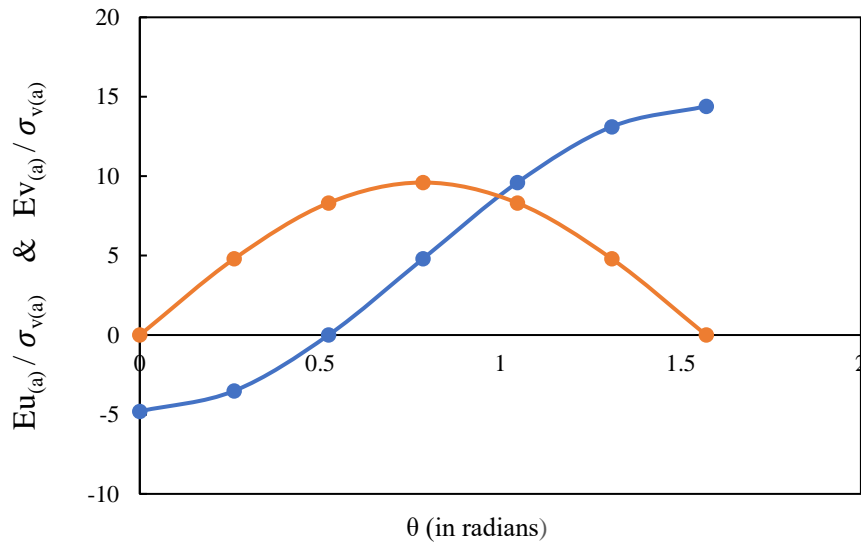


**Fig 3.4**  $\frac{Eu(a)}{\sigma_{va}}$  &  $\frac{Ev(a)}{\sigma_{va}}$  v/s  $\theta$

### 3.2.2 Bray (1967) Solutions

The Eqs. {(3.14) - (3.20)} are empirical in nature and are independent of  $\theta$ ,  $S_y$ ,  $v$ ,  $\frac{a}{r}$ . It only depends on the soil properties at which the tunnel is situated. Consequently, Trial curves can't be generated for Bray's Solution as within the scope of this study, it is assumed that the soil property is constant and the tunnel is situated in weak rock mass.

### 3.2.3 Pender (1980) Solutions

Solutions provided by Pender were divided into 2 cases *i.e.* Case III and Case IV. Case III deals with trial curves depicting stress functions and Case IV deals with trial curves depicting displacement function in terms of  $Eu$  and  $Ev$ .

**Case III:** Stress functions using Eqs. {(3.21), (3.22), (3.23)} are discussed in this case. Trial curves are obtained for:

$$1) \frac{\sigma_{\theta}}{S_y} \text{ v/s } \frac{r}{a}$$

$$2) \frac{\sigma_r}{S_y} \text{ v/s } \frac{r}{a}$$

Variation of various parameter and assumptions of the state of soil mass for the Eqs. {(3.21), (3.22), (3.23)} are identical to Case I which was already discussed.

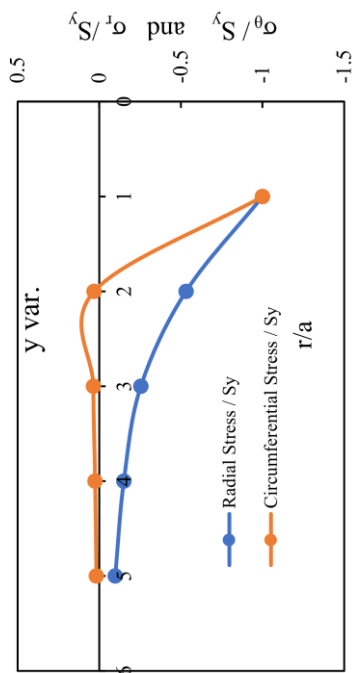
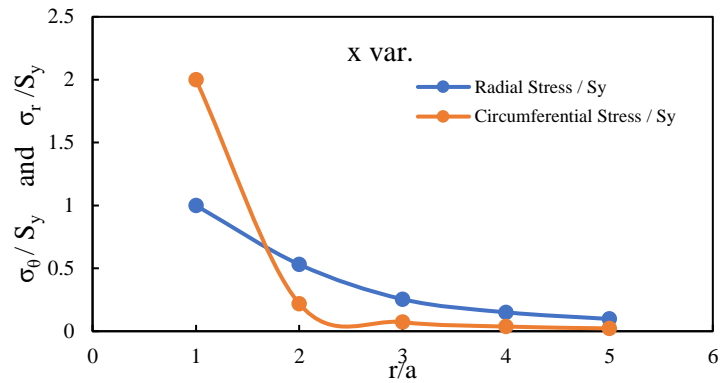
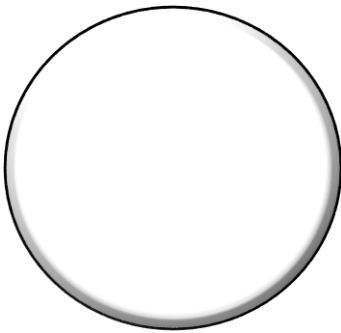


**Fig. 3.5** Variation of Radial and Circumferential Stresses along x and y direction

**Case IV:** Displacement functions using Eqs. {(3.24), (3.25)} are discussed in this case.

Curves are obtained for:

1.  $Eu(a) / \sigma_v(a) \text{ v/s } \theta$

2.  $E v(a) / \sigma_v(a)$  v/s  $\theta$

Assumptions made in the calculation for  $u$  and  $v$  (displacement component in  $x$  and  $y$  direction) using equations (3.24) and (3.25) are:

1. Poisson's ratio  $\nu = 0.2$
2. Vertical stress  $S_y = 20 \text{ kN/m}^2$ ;
3. Horizontal Stress  $S_x = 10 \text{ kN/m}^2$

Interestingly, it can be observed that even though the assumption of laterally applied confining stresses  $S_x = 10 \text{ kN/m}^2$  is made for both the cases (Case II and Case IV), the deformation considered for the present study is at the tunnel periphery i.e. at  $r = a$ . As this value of  $r$  is substituted to the Eqs. {(3.10), (3.11)}, it can be observed that the set of Eqs. reduce to a function dependent only on  $S_y$  (applied vertical stress) and is independent of  $S_x$ . Similarly, the Eqs. {(3.24), (3.25)} have been derived assuming  $S_x = 0 \text{ kN/m}^2$ .

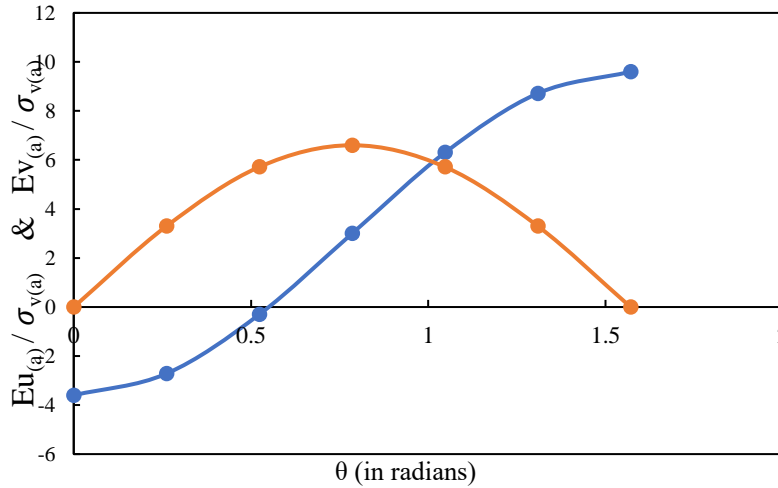


**Fig 3.6**  $\frac{E u(a)}{\sigma_{va}}$  &  $\frac{E v(a)}{\sigma_{va}}$  v/s  $\theta$

The trend of circumferential stress distribution in lateral direction as the  $r/a$  increases from 1 onwards, can be observed to decrease as the  $r/a$  increases upto  $r/a = 2$  and further attains a constant value beyond this point closely equal to the applied stress  $S_y$  (**Fig. 3.3**). This is according to Kirsch (1898) solution. But on the contrary, from **Fig.3.5** (Pender (1980)), it can be observed that the trend of circumferential stress distribution in lateral direction as the  $r/a$  increases from 1 onwards, can be observed to decrease with a higher rate than Kirsch (1898)

and reduces to 0 at some point after  $r/a = 2$ . Further, there is a slight increase in the circumferential stress which eventually becomes negligible and ultimately reduces to 0.

The trend of radial stress distribution in lateral direction as the  $r/a$  starts from 1 onwards, can be observed to increase as the  $r/a$  increases upto  $r/a = 2$  where it attains the peak and further gradually decreases and reduces to 0 (**Fig. 3.3**). This is according to Kirsch (1898) solution. But on the contrary, from **Fig.3.5** (Pender (1980)), it can be observed that the trend of radial stress distribution in lateral direction as the  $r/a$  increases from 1 onwards, can be observed to decrease gradually in opposed to Kirsch (1898) where radial stress increased and then decrease. Moreover, even after  $r/a = 5$ , the radial stress as calculated using Pender (1980) does not reduce to 0 and seems asymptotic in nature which would attain 0 at infinity.

The trend of circumferential stress distribution in vertical direction as the  $r/a$  increases from 1 onwards, can be observed to have a compressive nature  $r/a = 1$  (at the periphery) which increases as  $r/a$  increases and further attains a maximum value beyond  $r/a = 2$  and then decreases to 0 after  $r/a = 4$  (**Fig.3.3**). This is according to Kirsch (1898) solution. The similar trend is observed in **Fig.3.5** (Pender (1980)) for circumferential stress distribution vertically, the rate of increase of circumferential stress is higher in the latter than the former. Though, after  $r/a = 2$ , the behavior is identical.

The trend of radial stress distribution in vertical direction as the  $r/a$  starts from 1 onwards, can be observed to increase gradually as the  $r/a$  increases and we move away from the tunnel periphery. Though, it can be observed that the rate of increase is higher initially and reduces and ultimately becomes negligible after  $r/a = 5$  (**Fig. 3.3**). This is according to Kirsch (1898) solution. But on the contrary, from **Fig.3.5** (Pender (1980)), it can be observed that the trend of radial stress distribution in vertical direction as the  $r/a$  increases from 1 onwards, increases a compressive radial stress which is directed towards the tunnel center and increases as  $r/a$  increases and is asymptotic to the x axis in Fig. 3.5 (reduces to 0 at infinity).

In the deformation curves (**Fig. 3.4, Fig. 3.6**) The  $E_v$  curve is identical when obtained from both solutions but the  $E_u$  curve obtained using Pender (1980) can be observed to be skewed vertically as compared to  $E_u$  curve from Kirsch (1898) solution. In other words, the radial deformation obtained using Pender (1980) is smaller than radial deformation in case of Kirsch (1898).

## CHAPTER 4

---

### 4.1 Experimental Setup

Kumar, P. performed an experiment for the stress and deformation behavior under uniaxial conditions for circular tunnels. The experimental model involved circular tunnel with radius 3cm and 5cm made using Plaster of Paris. Perspex glass box with a central hole was used as the casting mould. The hole which is situated at some appropriate cover depth represented the circular tunnel. Elastic solution were obtained for stresses in the case of tunnels located near the surface and having initial stress gradient with depth (Mindlin(1940)). The results indicate that the influence of the surface on the stress distribution is not significant for depth to diameter ratio over 2 or 3. The influence of induced stresses in a tunnel is negligible after a radial distance of  $r = 4a$  (Obert, L. & Duvall (1967)). Hence beyond this limit of radial distance, we need not consider the displacements and stress variations.

The Perspex box was translucent in nature having a hole of radius 3cm and 5cm situated at the center (Fig. 3 (a)) and having an effective cover depth of 3cm and 5cm respectively from the top surface of the box. The box had detachable sides (edges) which can be removed after the hardening process is complete for easy retrieval of the model. PVC pipe was used to cast the circular tunnel which was fixed at the center through the circular hole. Plaster of Paris mixed with 60% by weight of water content was mixed and then poured into the Perspex box and allowed to set. After setting was complete, the detachable sides were then removed and the model was taken out. Also, the protruding edges of the PVC pipe were cut down to facilitate ease of handling.

For testing of the model, the mould was placed under the Uniaxial compression testing Machine at the Rock Mechanics Laboratory of Delhi Technological University, New Delhi and load was applied perpendicular to the axis of the tunnel. This case of loading simulated Uniaxial loading where only the vertical component of the loading is present and horizontal component is absent. Also, for determination of displacements in the tunnel, Strain Gauges were attached to the inside of tunnel at a distance of  $\frac{L}{4}$ ,  $\frac{L}{2}$  and  $\frac{3L}{4}$  from the face of the tunnel. The strain gauges were of 350 $\Omega$  resistance. Loading and strain gauge readings were tabulated with a time interval of 5s until model failure. Mean Strain of the 3 readings was considered for further analysis.

### 4.1.1 Perspex Box Design

The box was in the shape of a cuboid with central hole only on 2 opposite faces of the box. The assumption for the cuboidal shape of the box as opposed to any other shape was made as the length of the tunnel considered was longer as compared to the area of cross section which influenced the induced stresses in tunnel. The cuboidal shape of the model also facilitated the ease of testing under the universal compression testing machine as it provided a plane surface for the platens. The plane surface was also used for simulating load exerted on ground surface. The ground surface was assumed as distant boundary. Hence, all 3 adjacent sides of the model had different dimension. The radius of the circular tunnel was taken as 3cm in one model and 5cm in the other. Then the maximum radial distance of influence zone which is  $4a$  *i.e.*  $4 \times 3 = 12\text{cm}$  from the center of the tunnel in case of 3cm and  $4 \times 5 = 20\text{cm}$  in case of 5cm tunnel was provided. Hence the total vertical height of the box may be calculated as  $3 + 2 \times 3 + 12 = 21\text{cm}$ . Taking into account the manufacturing difficulties, the final chosen size of the Perspex box of dimension  $35\text{cm} \times 25\text{cm} \times 25\text{cm}$  for 3cm tunnel with a cover depth of 3cm

Similarly, the size of the box for 5cm diameter circular tunnel located at a cover depth of 5cm would be  $35\text{cm} \times 35\text{cm} \times 35\text{cm}$  but it would be cubical in shape. Fig. 3 shows the schematic diagram of the Perspex box and cross section

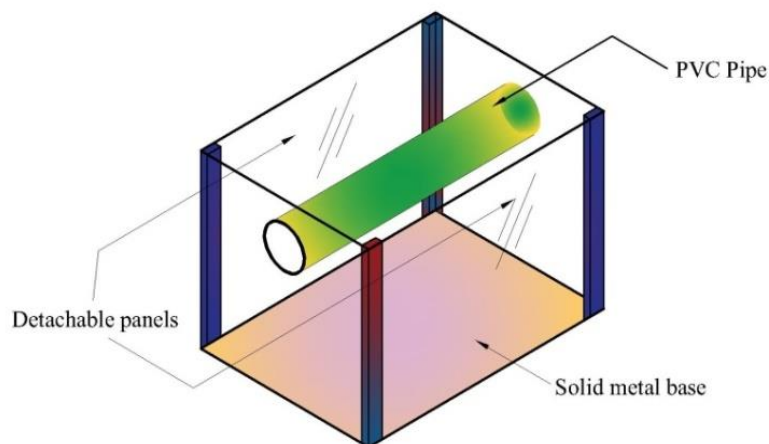


**Fig. 4.1** Schematic diagram of the Perspex box

For the deformation measurement, strain gauges are fixed at a distance of  $\frac{L}{4}$ ,  $\frac{L}{2}$  &  $\frac{3L}{4}$  from the tunnel opening face, where  $L$  is the length of the tunnel, which is taken as 35cm.

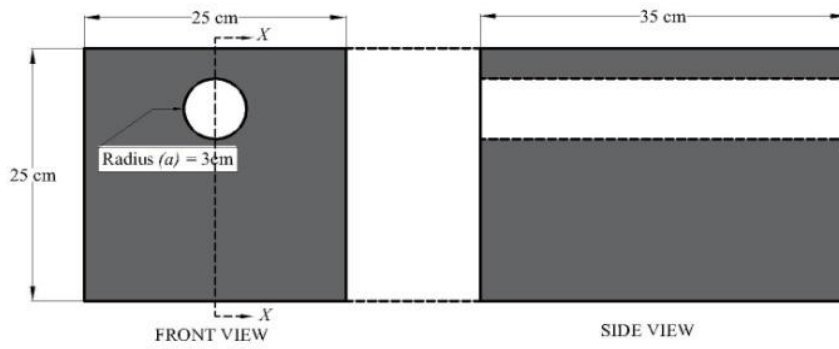


**Fig. 4.2** Front View and cross section at X-X

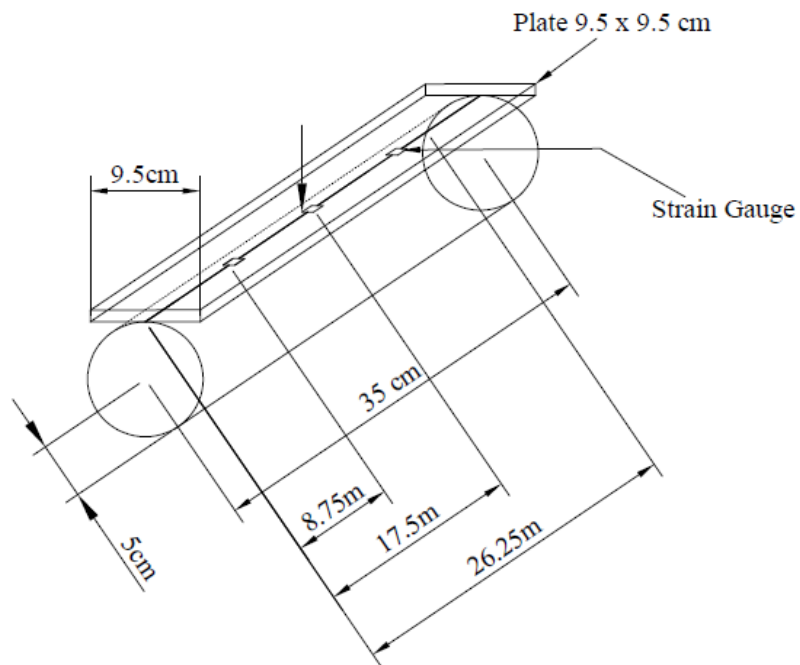


**Fig. 4.3** Load Setup of a circular tunnel model



## CHAPTER 5

---

### 5.1 Conduction of experiment

The model test performed was by Kumar, P (2017). The loading was applied by the Uniaxial Compression testing machine at every 5 sec interval and corresponding Strain gauge readings were noted down. Mean Strain was calculated for each time interval. Readings were considered until the specimen model failed and there was a sudden decrease in the load in the subsequent readings. The load at which the failure of model took place was termed as Ultimate Load. The testing was performed for both the models. The output results from experiments were Mean strain v/s Time and Load v/s Time plots. These results have been directly acquired from the test conducted by Kumar, P. for the purpose of further analysis and study.

### 5.2 Analytical Results

For the calculation of stresses as well as deformations, data adopted are listed below:

**Table 5.1** Maximum induced stress values

Model	S <sub>y</sub> (MPa)
3cm Unlined	2.78
5cm Unlined	3.59

Nomenclature used:

S<sub>y</sub> = induced vertical stress

S<sub>y</sub> can be calculated by using definition of simple stress from mechanics of solids

=  $\frac{\text{Load acting}}{\text{Area normal to the loading plane}}$  . Considering the load at Failure point and Normal area

as area of the loading platens used i.e. 95mm x 95mm.

#### 5.2.1 Kirsch (1898) Solutions

Consider a circular tunnel. Due to Symmetry of shape, we would consider only 1<sup>st</sup> Quadrant of the circle ( $0^{\circ} \leq \theta \leq 90^{\circ}$ ). Using Eqs. {(3.4), (3.5), (3.6)} for stress calculation and Eqs. {(3.10), (3.11)} for deformation calculation.  $r$  i.e. the radial distance has been varied from minimum of  $a$  to a maximum distance of  $4a$  (Obert, L. & Duvall (1967)).

**Table 5.2** Nomenclature

Quantity Represented by	$\sigma_r$	$\sigma_\theta$	$\tau_{r\theta}$	$E_u$	$E_v$
	$p$	$q$	$r$	$t$	$w$

**Note:**  $p$ ,  $q$  and  $r$  is expressed in MPa;  $t$  and  $w$  are expressed in N/mm.

**Table 5.3** Stress values for 3cm model

$r/a$ $\theta$	1			2			3			4		
	$p$	$q$	$r$	$p$	$q$	$r$	$p$	$q$	$r$	$p$	$q$	$r$
$0^0$	0	8.34	0	0.782	3.388	1.824	0.405	2.981	1.643	0.244	2.883	1.547
$30^0$	0	5.56	0	0.912	2.563	0.912	0.822	2.261	0.821	0.774	2.180	0.773
$45^0$	0	2.78	0	1.042	1.738	0	1.238	1.541	0	1.303	1.476	0
$60^0$	0	0	0	1.173	0.912	-0.91	1.656	0.822	-0.82	1.833	0.774	-0.77
$90^0$	0	-2.8	0	1.303	0.087	-1.82	2.072	0.102	-1.26	2.361	0.071	-1.55

**Table 5.4** Stress values for 5cm model

$r/a$ $\theta$	1			2			3			4		
	$p$	$q$	$r$	$p$	$q$	$r$	$p$	$q$	$r$	$p$	$q$	$r$
$0^0$	0	10.77	0	1.01	4.375	2.356	0.523	3.849	2.122	0.315	3.723	1.998
$30^0$	0	7.18	0	1.178	3.309	1.177	1.061	2.919	1.061	0.999	2.815	0.999
$45^0$	0	3.59	0	1.346	2.243	0	1.599	1.990	0	1.683	1.907	0
$60^0$	0	0	0	1.514	1.178	-1.17	2.138	1.061	-1.06	2.366	0.999	-0.99
$90^0$	0	-3.59	0	1.683	0.112	-2.36	2.676	0.131	-2.12	3.050	0.091	-1.99

For displacement calculations, Assuming  $\nu$  (Poisson ratio) = 0.2; E (Young's modulus) = 1800MPa.

**Table 5.5** Displacement values

$\theta$	3cm tunnel		5cm tunnel	
	$t$	$w$	$t$	$w$
$0^0$	-80.06	0	-172.32	0
$30^0$	0	138.675	0	298.466
$45^0$	80.06	160.128	172.32	344.64
$60^0$	160.13	138.675	344.64	298.467
$90^0$	240.192	0	516.96	0

### 5.2.2 Bray (1967) Solutions

Eqs. (11) and (12) are used for stress calculation. 2 cases have been considered to identify the differences in the results. Case (i), where the adjacent soil mass have been considered as soft clay. In Case (b), medium has been considered as weak rock (having Uniaxial Compressive strength  $< 50$  kPa (Záruba and Mencl (1974)). Even though, within the scope of this study , we are to consider only tunnel situated in rock mass, it is in the interest to determine the differences among the results provided by Bray(1967) solutions in case of soil as well as rock. The property of soil/rock mass is adopted from the GEOL manual which states the general properties of materials, soil and rock properties.

#### Case (i) : Soft clay as surrounding soil mass

Adopt  $\phi = 20^0$ ,  $c$  = cohesive strength = 48 kPa

Using Eqs. {(3.16 - 3.19)} and substituting in Eqs. {(3.14), (3.15)}

We get  $\sigma_r = 115.25$  MPa ;  $\sigma_\theta = 56.50$  MPa

#### Case (ii) : Weak rock as surrounding rock mass $\phi = 30^0$

Using Eqs. {(3.16 - 3.19)} and substituting in Eqs. {(3.14), (3.15)}

We get  $\sigma_r = -132.64$  MPa;  $\sigma_\theta = -44.21$  MPa

Bray's Solutions has a number of limitations in determination of stresses around a circular tunnel. The solutions provided by Bray are purely a function of shear strength parameters of

the soil mass ( $c$ ,  $\phi$ ) and radius of tunnel only ( $r$ ). Hence, it considers the soil mass present in the nearby vicinity of the tunnel as the prime load imposing element which induces the stresses and does not take into account the change in stress as the radial distance from the tunnel surface varies. Also, solution for shear stress was not provided. On the other hand, in case the tunnel is located at soil mass, it provides a clear demarcation of the extent to which plastic zone exists and also gives formulae to calculate the radius of plastic zone.

### 5.2.3 Pender (1980) Solution

Using Eqs. {(3.21), (3.22), (3.23)} for stress calculation and Eqs. {(3.24), (3.25)} for deformation calculation.

**Table 5.6** Stress values for 3cm model

$r/a$	1			2			3			4		
$\theta$	$p$	$q$	$r$	$p$	$q$	$r$	$p$	$q$	$r$	$p$	$q$	$r$
$0^0$	0	5.56	0	0.80	0.60	0	0.405	0.2	0	0.244	0.103	0
$30^0$	-0.7	3.5	-1.2	0.22	0.47	0.376	0.126	0.176	0.219	0.078	0.095	0.136
$45^0$	-1.4	1.39	-1.4	-0.35	0.34	0.434	-0.15	0.151	0.253	-0.09	0.087	0.157
$60^0$	-2.0	-0.7	-1.2	-0.91	0.21	0.376	-0.43	0.126	0.219	-0.25	0.078	0.136
$90^0$	-2.8	-2.8	0	-1.48	0.08	0	-0.70	0.102	0	-0.42	0.071	0

**Table 5.7** Stress values for 5cm model

$r/a$	1			2			3			4		
$\theta$	$p$	$q$	$r$	$p$	$q$	$r$	$p$	$q$	$r$	$p$	$q$	$r$
$0^0$	0	7.18	0	1	0.785	0	0.522	0.259	0	0.315	0.133	0
$30^0$	-0.9	4.50	-1.6	0.28	0.617	0.486	0.164	0.227	0.283	0.101	0.122	0.17
$45^0$	-1.8	1.80	-1.8	-0.5	0.448	0.561	-0.20	0.195	0.327	-0.11	0.112	0.20
$60^0$	-2.7	-0.9	-1.6	-1.2	0.280	0.486	-0.55	0.164	0.283	-0.33	0.102	0.17
$90^0$	-3.6	-3.6	0	-1.9	0.112	0	-0.91	0.132	0	-0.54	0.091	0

**Table 5.8** Displacement values

$\theta$	3cm tunnel		5cm tunnel	
	$t$	$w$	$t$	$w$
$0^0$	-60.05	0	-129.24	0
$30^0$	-5	95.34	-10.77	205.196
$45^0$	50.04	110.88	107.70	236.94
$60^0$	105.084	95.34	226.17	205.196
$90^0$	160.128	0	344.64	0

The analytical solutions provided by Bray (1967) does not provide significant information about the point of application of the determined stresses but only gives a general idea of the nature of stresses. In other words, the stresses calculated using Bray (1967) solutions are independent of  $\theta$  which is the angle taken anticlockwise from the positive abscissa. The Bray (1967) solution does not consider the effect of cover depth. It is applicable to weak soil mass. If we use the solutions for stress determination in case of circular tunnel situated in strong rock whose cohesion and angle of friction is known, the results are not satisfactory. Bray (1967) did not provide any solution to determine the displacements on the tunnel periphery. The solutions set provided by Bray (1967) cannot be compared with that of Kirsch (1898) and Pender (1980) due to above stated limitations. Hence the solutions provided in Bray (1967) are inferior when compared with Kirsch (1898) or Pender (1980).

### 5.3 Graphical Comparison of Analytical Results

#### 5.3.1 Stress comparison

As per the Tables {(5.3), (5.4)} and Tables {(5.6), (5.7)} the stress coordinates were determined and it is mapped graphically by plotting the stresses on the quadrant I of the tunnel section.

The color codes used for stresses are as follows:

$$\sigma_r - \text{red circle} \quad \sigma_\theta - \text{blue circle} \quad \tau_{r\theta} - \text{yellow circle}$$

**Note:** The colour codes used in both the Cases are same. The scale considered for Fig.4 and Fig.5 are 1:1.

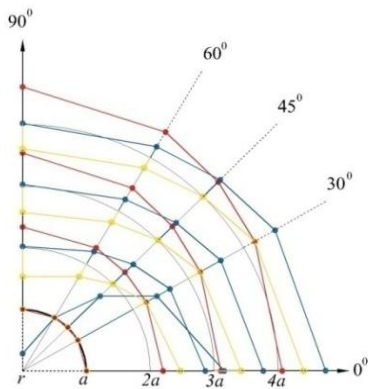
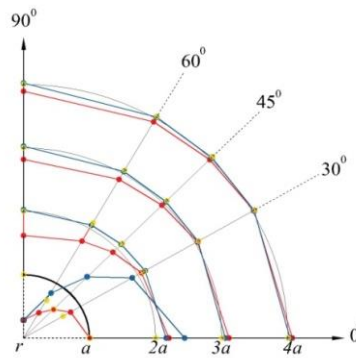


**Fig. 5.1** (a) 5cm Tunnel (Table 5.4)



(b) 5cm Tunnel (Table 5.7)

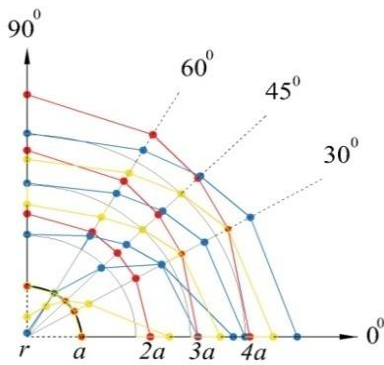
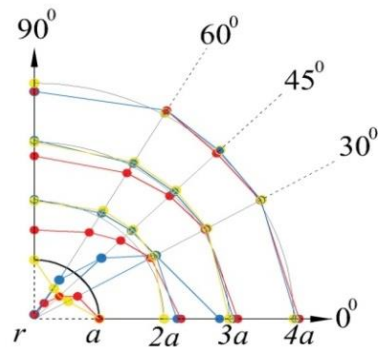


**Fig. 5.2** (a) 3cm Tunnel (Table 5.3)





(b) 3cm Tunnel (Table 5.6)

The stresses determined by Eqs. {(3.4), (3.5), (3.6)} and Eqs. {(3.21), (3.22), (3.23)} have higher magnitude as the size of tunnel diameter increases. This is due to the fact that the equations are in direct proportion to  $\left[ \frac{a}{r} \right]$  where 'a' is the radius of the tunnel. Radial stress and Shear stress are absent at  $r = a$  i.e. at the periphery irrespective of size of the tunnel.

### 5.3.2 Deformation Comparison

The color codes in both the Cases are same. The scale considered for Fig.11 and Fig.12 is

1:1. Color code:  $u$  -   $v$  - 

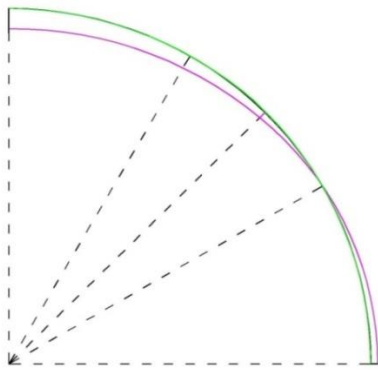
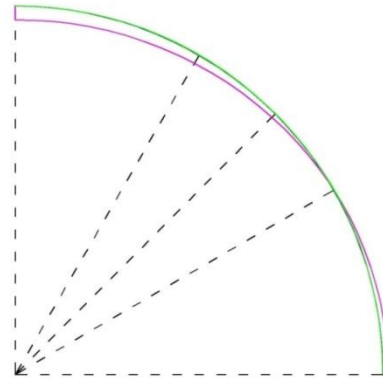


**Fig. 5.3** (a) 5cm Tunnel (Table 5.5)



**(b)** 5cm Tunnel (Table 5.8)

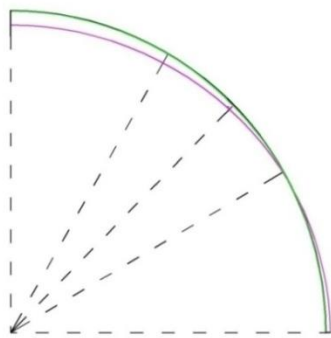
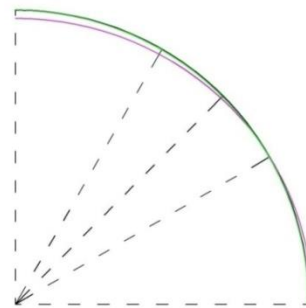


**Fig. 5.4** (a) 3cm Tunnel (Table 5.5)



**(b)** 3cm Tunnel (Table 5.8)

In Kirsch(1898) solutions, radial and tangential displacements increase with distance from the opening. Displacements would be largest where the stresses are applied.  $v$  would be greatest at the surface, although  $u$  would still be greatest at the tunnel periphery.

Deformation of a tunnel may result in settlement of the ground surface. Generally, two basic deformation mechanisms occur when we discuss about deformation of a tunnel. Firstly, a uniform radial displacement representing the ground loss that may occur during the construction. And secondly, ovalization of tunnel. Hence total deformation is the sum of both cases, but within the scope of this study, the phenomenon of surface settlements is not taken into account. But, within the limits of this study, only peripheral displacements are accounted.

## CHAPTER 6

### 6.1 Analytical result curves

Graphs depicting the variation of radial, circumferential and shear stresses with time for Eqs. {(3.4), (3.5), (3.6)} are as follows:

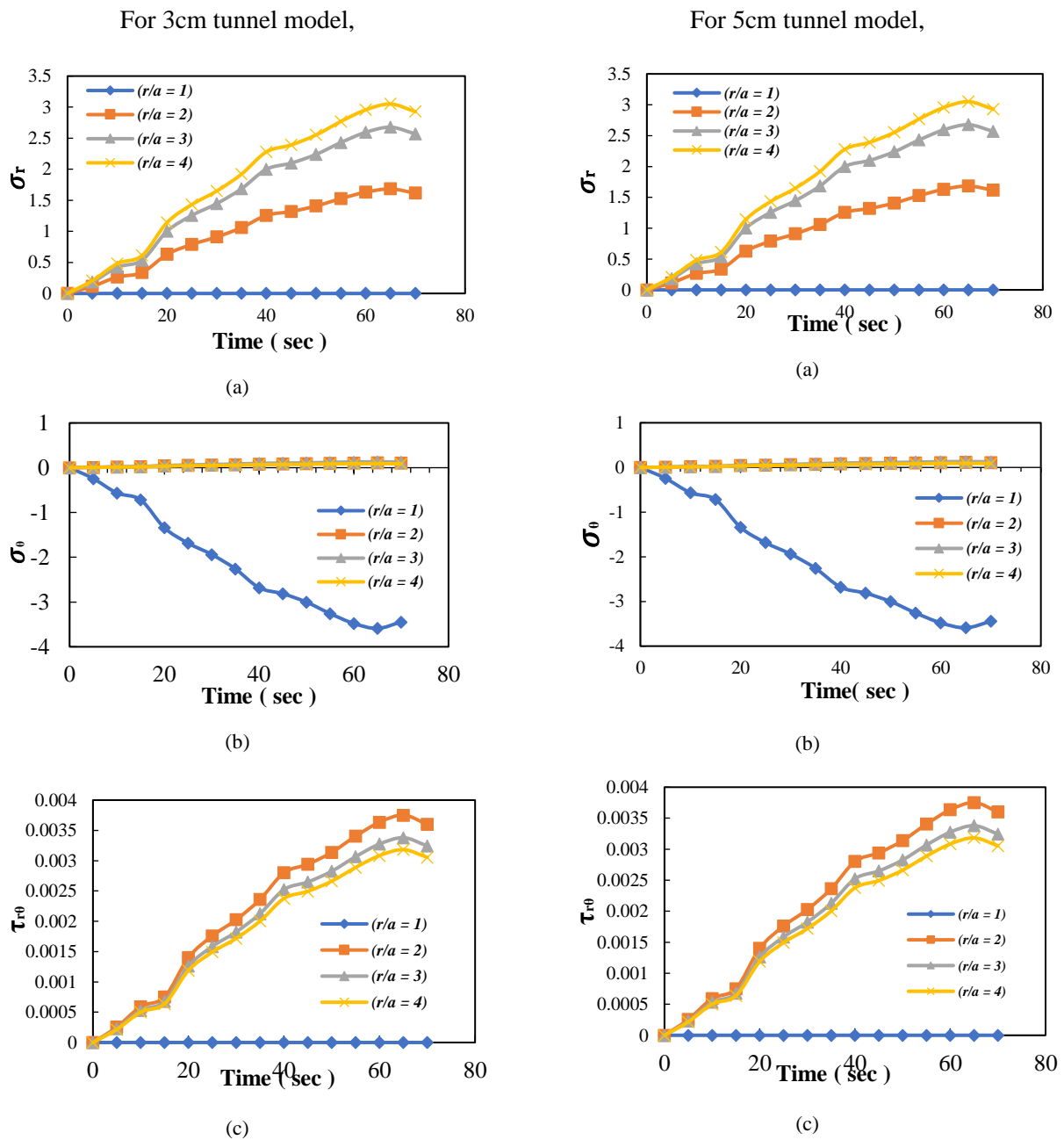


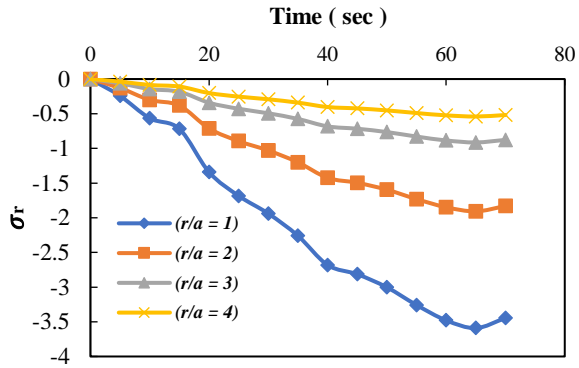
**Fig.6.1** (a)  $\sigma_r$  v/s t (sec) (b)  $\sigma_\theta$  v/s t (sec)  
(c)  $\tau_{r\theta}$  v/s t (sec)

**Fig.6.2** (a)  $\sigma_r$  v/s t (sec) (b)  $\sigma_\theta$  v/s t (sec)  
(c)  $\tau_{r\theta}$  v/s t (sec)

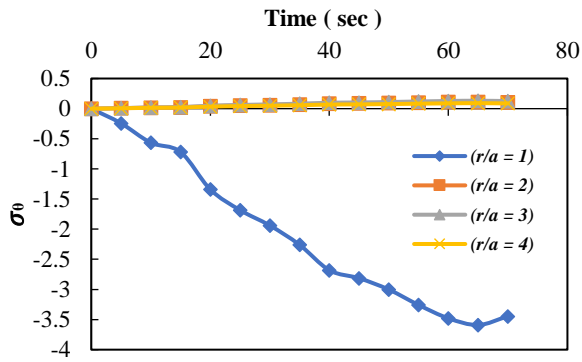


Graphs depicting the variation of radial, circumferential and shear stresses with time for Eqs. {(3.21), (3.22), (3.23)} are as follows:

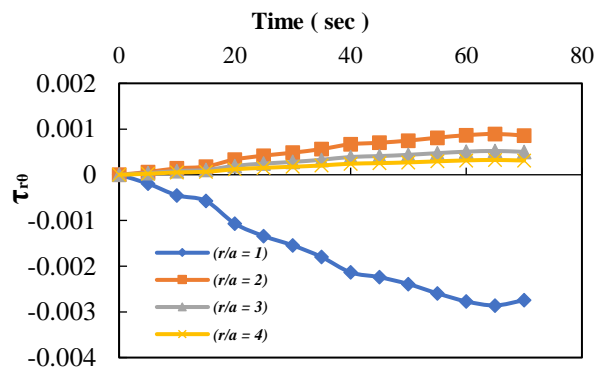
For 3cm Tunnel model,



(a)



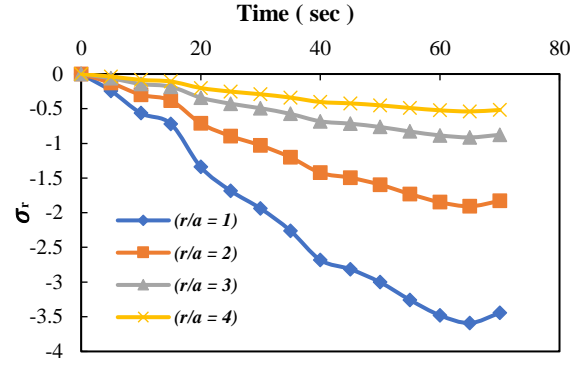
(b)



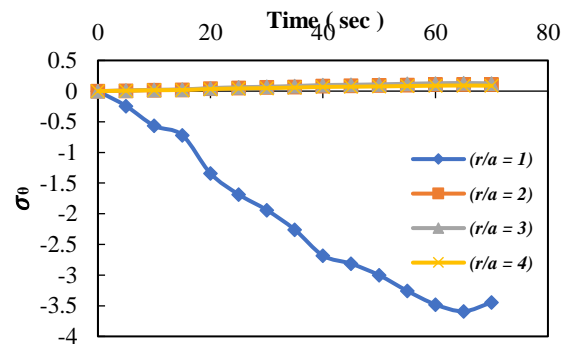
(c)

**Fig.6.3** (a)  $\sigma_r$  v/s t(sec) (b)  $\sigma_\theta$  v/s t(sec)  
(c)  $\tau_{r\theta}$  v/s t (sec)

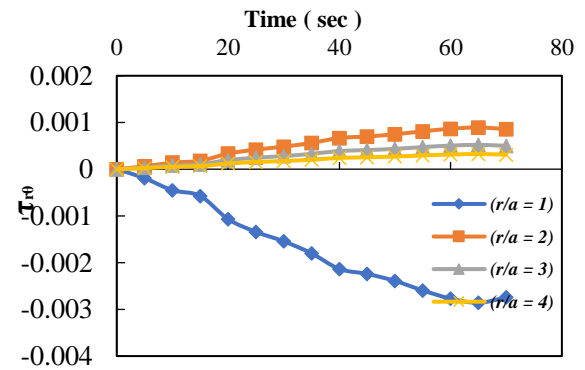
For 5cm Tunnel model,



(a)



(b)



(c)

**Fig. 6.4** (a)  $\sigma_r$  v/s t(sec) (b)  $\sigma_\theta$  v/s t(sec)  
(c)  $\tau_{r\theta}$  v/s t (sec)

There is an increase of 29.13% in circumferential stress at the periphery. The maximum stress magnitude is observed at the abscissa ( $0^0$ ) for all stress entities irrespective of size of the tunnel. Maximum increase in radial stress is observed as 29.13% where as 29.11% increase is observed in circumferential stress and 29.15% in shear stress across all radial distances till influence zone. Hence, it can be aptly said that there is an increase in stress magnitude by 29% for an increase in the tunnel radius by 66.67%.

## 6.2 Stress v/s Strain

Stress v/s Strain curves are obtained for 3.1.1 (denoted by Kirsch(1898)) and 3.1.3 (denoted by Pender(1980)). Graphs indicating the interdependency of stress at the point of application of load with strain experienced at the point which have been obtained experimentally are as follows:

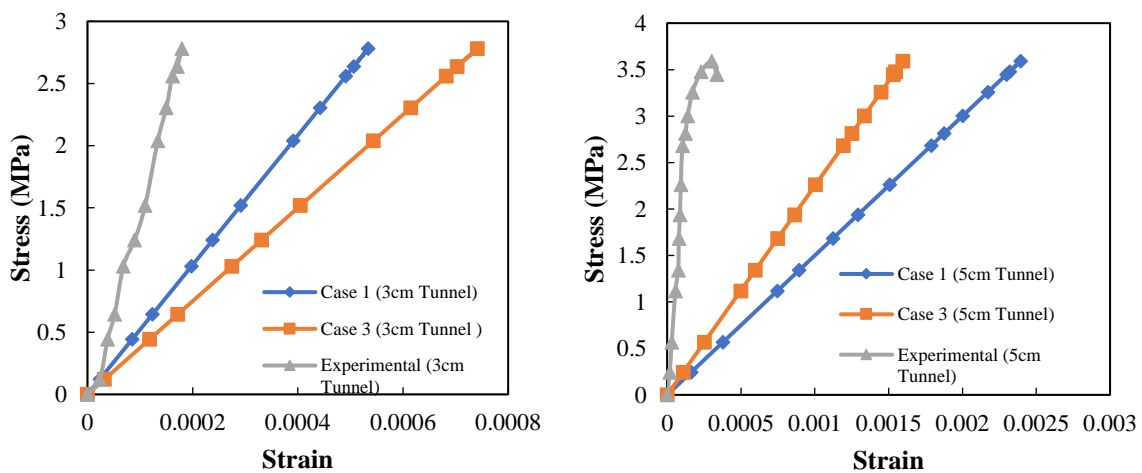


**Fig.6.5** (a) Stress v/s Strain trend for 3cm tunnel (b) Stress v/s Strain trend for 5cm tunnel

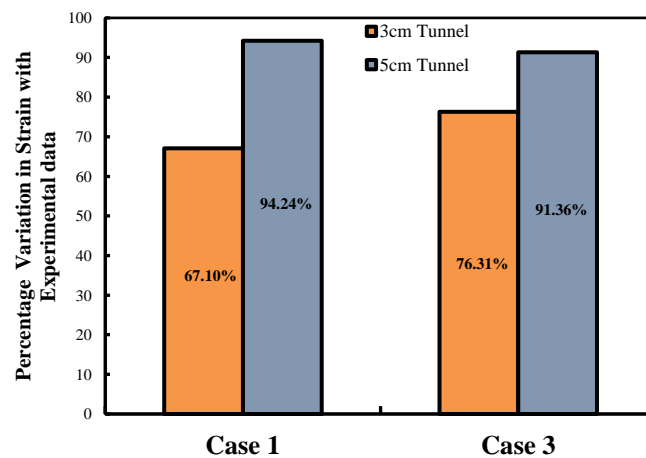


**Fig.6.6** Percentage variation in Strain with experimental readings

Fig.7.5 (a) shows the trend for stress v/s strain for 3cm tunnel model. It can be seen that for the experimental curve, the stress increases faster than the strain developed (as the slope is steepest) as compared to Kirsch(1898) solutions and Pender(1980) solution curves. Also, Kirsch(1898) solutions curve is steeper as compared to Pender(1980) solution, hence it can be concluded that for tunnels of smaller diameter, Kirsch(1898) solutions is more realistic than Pender(1980) solution. Also, analytical curves are follows linear model which is due to the fact that solutions provided in Kirsch(1898) solutions and Pender(1980) solutions for stresses are linearly varying with strain.

Fig. 7.5 (b) shows the trend for stress v/s strain for 5cm tunnel model. It can be seen that for the experimental curve, the curve is parabolic in nature whereas, both the analytical curves (Kirsch(1898) and Pender(1980) solution) are linear model. This is as per the fact that as these curves are obtained for the peripheral stress system, the terms in Eqs. {(3.4), (3.5), (3.6)} and Eqs. {(3.21), (3.22), (3.23)} reduces to linear function and depends only on the stress applied at the distant boundary  $S_y$  and  $\theta$  and are independent of non-linear higher order terms like  $[\frac{a}{r}]^2$ ,  $[\frac{a}{r}]^3$  etc. Another important observation is that, the Kirsch(1898) curves is flatter as compared to Pender(1980). Hence, it can be concluded that, for tunnels of larger diameter, Pender(1980) provides more realistic results

In Pender(1980) solutions, as the size of the tunnel increases, the same trend of increase in the stress magnitude is observed as in Kirsch(1898) solutions. However, the radial and shear stress are not absent at the tunnel periphery as it was in Kirsch(1898) solution. Increase of 29% in radial stress, 29.13% in circumferential stress and 29.50% in case of shear stress is observed as the tunnel radius increases by 66.67%.

Comparing Kirsch(1898) solution and Pender(1980) solution, it can be seen that as we move away from the tunnel periphery, the stress magnitudes decrease which is trivial as the influence of loads decreases and ultimately vanishes after  $r = 4a$ . However, the rate of decrease in the magnitude of stresses is greater in Pender(1980) solution as opposed to Kirsch(1898) solution.

### 6.3 Deformation Profile

The deformation is measured indirectly with the help of Strain Gauges. 3 foil type strain gauges (NIE Phenolic Gate Resistance -  $350 \pm 0.3 \Omega$ , Gauge factor =  $2.11 \pm 1\%$ , Temperature Compensation as  $11 \times 10^{-6} / ^\circ\text{C}$ , Gauge length = 3.175mm) are placed at a distance of  $\frac{L}{4}$ ,  $\frac{L}{2}$  and  $\frac{3L}{4}$  from the face of the tunnel. Load and strain gauge readings were noted with a time interval of 5s until failure of the model. Mean Strain of the 3 readings was consider for further analysis. The deformed profile as obtained from Table {5.5} and Table {5.8} are as follows:

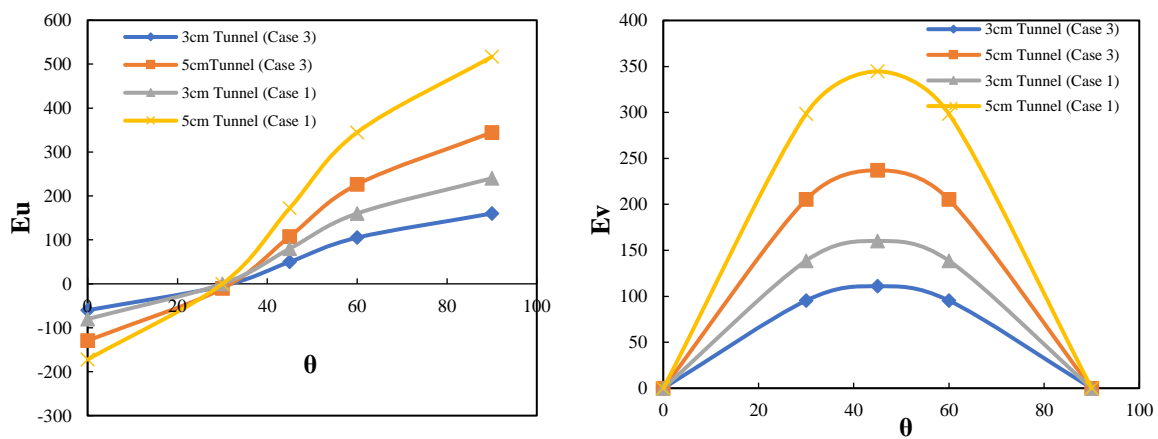


**Fig.6.7** (a)  $E_u$  v/s  $\theta$

(b)  $E_v$  v/s  $\theta$

Above curves show the variation of  $E_u$  and  $E_v$  with  $\theta$  ( $\theta$  varies from  $0^\circ$  to  $90^\circ$ ).

The displacement at the point of loading calculated as per Kirsch(1898) solution and Pender(1980) solution differ by 50% (maximum) and 33.33% (minimum) in case of  $u$  (radial displacement) and 45.45% (both minimum and maximum) in case of  $v$  (tangential displacement). From Fig. 7.5, it can be inferred that lesser variation in Strain values are observed for Kirsch(1898) solution than Pender(1980) solution. Hence Kirsch(1898) solution displacement results are superior to Pender(1980) solution. Also, variation in Strain value is lower when the size of the tunnel is smaller. Therefore, it can be stated that as the size of the tunnel increases, the degree of accuracy decreases to a large extent. This can be seen from Fig. 7.6 wherein for 3cm tunnel, the percentage variation varies from 67% (Kirsch(1898) solutions) to 76% (Pender's solution) and percentage variation varies from 94% (Kirsch(1898) solutions) to 91% (Pender(1980) solution). Hence, for bigger tunnels, Kirsch(1898) solutions shows larger deviation from the experimental data than Pender's solution.

## CHAPTER 7

---

### 7.1 Conclusion

The major results obtained from the present study can be emphasized as follows:

- 1) Kirsch(1898) displacement solutions are not relevant for the case of tunnel excavation but in cases where stresses in the ground surface change after the tunnel excavation has been completed.
- 2) Further investigations are required to establish the changes of surface movement effects in the stresses computed analytically in Kirsch(1898) or Pender(1980) solution.
- 3) Bray(1967) Solutions are relevant for tunnels located in soft soil and it greatly overestimates the magnitudes of radial and circumferential stress in case of rock mass.
- 4) Both solutions (Kirsch(1898) and Pender(1980)) have limitations and hence are to be used only for primary estimation of stresses and displacements.
- 5) For tunnels of smaller diameter, Kirsch's solution is more preferable and for larger diameter tunnels, Pender's solution is more preferable.

## References

- Barton N, Grimstad E., Aas G, Opsahl OA, Bakken A., Pesersen L, Johansen ED (1992) Norwegian method of tunnelling, focus on nor-way world tunnelling June/August
- Barton N, Licn R, Lunde J (1974) Engineering classification of rock masses for design of tunnel support, *Rock mech.* 6(4):189–236
- Brady B.H.G, Brown E.T. (1993) *Rock Mechanincs for Underground Mining*, 2<sup>nd</sup> ed. Chapman & Hall, London, UK
- D. Bernaud, Rousset G. (1996) The “NEW IMPLICIT METHOD” for tunnel analysis. *International Journal for numerical and Analytical methods in geomechanics*, Vol. 20(9):673–690
- Gercek H. (1991) Stresses around tunnels with arched roof, *Proc.7<sup>th</sup> Int. Cong. On Rock Mechanics, ISRM, Balkema, Rotterdam, Netherlands*, Vol.2:1297–1299
- Gercek H. (1997) An elastic solution for stresses around tunnels with conventional shapes, *Int. J. Rock Mech. & Min. Sci.*, Vol.34:3-4, Paper No.096
- Greenspan M. (1994) Effect of a small hole on the stresses in a uniformly loaded plate, *Q. J. Appl. Math.*, Vol.2:60–71
- Guo H. (2019) A Review of Metro Tunnel Construction Methods IOP Conf. Ser.: Earth Environ. Sci. 218 / 012110
- Heinz Konietzky, H. H. (2019) Simple analytical solutions for underground circular and elliptical openings, *Geotechnical Institute, TU Bergakademie Freiberg*, 1:1–14
- Inglis C.E. (1913) Stresses in a plate due to the presence of cracks and sharp corners, *Trans. Inst. Naval Arch.*, Vol.55:219–230
- Kirsch G. (1898) Die Theorie der Elastizität und die Bedürfnisse der Festigkeitslehre, *Zeit. Ver. Deut. Ing. J.*, Vol.42:797–807
- Lunardi P (2000) Design and construction of tunnels ADECORS approach. *Tunnels and tunnelliing international special supplement*
- Malvern L.E. (1969) *Introduction to the Mechanics of a Continuous Medium*, Prentice Hall, Englewood Cliffs, NJ, USA
- M. J. Pender (1980) Elastic solutions for a deep circular tunnel, *Technical Notes*, 216–222
- Negro, A., de Quieroz, P.I.B. (2000) Prediction and performance: A review of numerical analysis for tunnels, *Geo. Aspects of Underground Const. in soft ground*, *Int. Society for Soil Mech. and Geot. Engg.*, Balkema, Rotterdam, 409–418
- Obert L., Duvall W.I., Merrill R.H (1960) Design of underground openings in competent rock, *US Bureau of Mines Bulletin*, pp.587
- Obert, L., Duvall (1967) *Rock mechanics and the design of structures in rock*, John Wiley & Sons, Wiley, pp.94–111
- Phadke V., Titirmare N. (2017) Construction of tunnels by New Austrian Tunneling method (NATM) and by Tunnel Boring Machine (TBM), *Int. J. of Civil Eng.*, Vol. 6(6):25– 36

Raghvendra V., Saravana Raja Mohan, K. (2014) Dynamic Analysis of tunnels in Urban areas with and without support systems, *Int. J. of Eng. Research and Technology*, Vol. 3(5):270–275

Wang JY (1997) An important tool to construct underwater tunnels; segment immersing method. *Word Tunn* 1:65–67

Xiao F, Guo HW, Guo JY (2009) Brief description on the New Austrian method. *Shanxi Archit* 35(4):284–285

Záruba, Q., Mencl, V. (1974) *Engineering Geology*, Praha, Czech, Academia